Single-particle potential in dense nuclear matter

R. B. Wiringa
Physics Division, Argonne National Laboratory, Argonne, Illinois 60439
(Received 10 August 1988)

The single-particle potential in nuclear matter is calculated microscopically for several Hamiltonians for densities ranging from 0.1 to 0.5 fm^{-3}. These Hamiltonians include nucleon-nucleon potentials fit to scattering data and three-nucleon potentials fit to the binding energies of few-body nuclei and saturation properties of nuclear matter. The single-particle potential is a key ingredient in Boltzmann-Uehling-Uhlenbeck simulations of heavy-ion collisions. Parametrizations of the density and momentum dependence of the single-particle potential that may be useful in such simulations are discussed and compared to phenomenological prescriptions currently in use.

The Boltzmann-Uehling-Uhlenbeck (BUU) equation provides one of the chief methods for simulating heavy-ion collisions microscopically.[1] The BUU equation is a transport equation which includes stochastic collisions between individual nucleons, particle production, effects of the Pauli principle, and propagation between collisions controlled by a mean field. The mean field, or single-particle potential, is a functional derivative of the interaction energy for the system, and is thus directly related to the nuclear matter equation of state. The single-particle potential has frequently been assumed to take some relatively simple form, such as the Skyme parametrization:

$$U(\rho)=a(\rho/\rho_0)+b(\rho/\rho_0)^{\sigma} . \tag{1}$$

Attempts to explain pion production data[2] and collective flow[3] with this form led to the conclusion that the equation of state must be very stiff,[4] in disagreement with microscopic calculations based on Hamiltonians fit to nucleon-nucleon scattering data[5] and attempts to deduce the equation of state from supernova simulations.[6]

The momentum dependence of the real part of the optical potential is neglected in the parametrization of Eq. (1). Several groups have started to study the effect of the momentum dependence of $U(\rho,k)$ in BUU simulations.[7,8] They find that an equation of state with an incompressibility of $\sim$215 MeV and a reasonable $U(\rho,k)$ can fit current heavy-ion collision data as well as a stiff equation of state without momentum dependence.

In this paper I report microscopic calculations of the single-particle potential for several realistic Hamiltonians that fit nucleon-nucleon scattering data, few-body nuclear binding energies, and nuclear matter saturation properties. The ground-state properties of these models were recently studied by Wiringa, Fiks, and Fabrocini (WFF).[9] The models are also in good agreement with a variety of neutron star data, although they may be too stiff to produce supernovae explosions by a prompt shock mechanism. I also discuss parametrizations for $U(\rho,k)$ which could be used in BUU simulations of heavy-ion collisions.

The calculation of $U(\rho,k)$ uses a method developed by Friedman and Pandharipande[10] (FP) that is consistent with the variational ground-state calculations of WFF. The energy $e(\rho,k)$ of a quasiparticle or quasihole state is assumed to have the usual form:

$$e(\rho,k)=\frac{\hbar^2}{2m}k^2+U(\rho,k) . \tag{2}$$

The energy at the Fermi surface is given by a functional derivative of the energy density of the system with respect to changes in density,

$$e(\rho,k_F)=E_0(\rho)+\rho\frac{\partial E_0(\rho)}{\partial\rho} , \tag{3}$$

where $E_0(\rho)$ is the ground-state expectation value of the energy per nucleon. In variational calculations this expectation value is computed with a wave function

$$\Psi_0=\left[S\prod_{i<j}F_{ij}\right]\Phi[(n)k=n_0(k)] , \tag{4}$$

where Φ is a Fermi-gas wave function with occupations $n(k)$ acted on by a symmetrized product of two-body correlation operators F_{ij}. Here $n_0(k)$ denotes the occupation of a filled Fermi sea, i.e., $n_0(k<k_F)=1$ and $n_0(k>k_F)=0$.

The FP procedure assumes that single quasiparticle or quasihole states can be well described by simply altering the occupation $n(k)$, without changes to F_{ij}. The quasiparticle or quasihole energy as a function of momentum for a fixed density is then obtained by taking a functional derivative of the energy density with respect to changes in $n(k)$. For quasiparticle (hole) energies $n(k)$ is altered by removing a small fraction x of the particles from a thin spherical shell at $k=k_F$ ($k=y<k_F$) in momentum space and promoting them to a thin spherical shell at momentum $k=y>k_F$ ($k=k_F$). This leads to

$$e(\rho,y)=e(\rho,k_F)\pm\frac{1}{x}(E(\rho,x,y)-E_0(\rho)) , \tag{5}$$

where $E(\rho,x,y)$ is the energy expectation value evaluated with $\Psi_v[n(k)=n_0(k)\pm x(\delta_{k,y}-\delta_{k,k_F})]$, and the plus (minus) sign refers to particle (hole) states.

Friedman and Pandharipande used this method to calculate the single-particle potential for the Urbana v_{14} plus three-nucleon interaction (UV14 plus TNI) model Hamiltonian[11] at densities from $\frac{1}{4}\rho_0$ to ρ_0. They found good agreement with optical potential analyses of nucleon-nucleus scattering data. In this paper I calculate $U(\rho,k)$ for densities up to $3\rho_0$ for the UV14 plus TNI model and for two Hamiltonians of the form

$$H=\sum_i \frac{-\hbar^2}{2m}\nabla_i^2+\sum_{i<j} v_{ij}+\sum_{i<j<k} V_{ijk} , \quad (6)$$

where v_{ij} is either the Urbana v_{14} (UV14) or Argonne v_{14} (AV14) nucleon-nucleon potential[12] and V_{ijk} is the Urbana model VII (UVII) three-nucleon potential.[13]

The UV14 plus TNI model attempts to simulate the effect of three-nucleon interactions by adding phenomenological density-dependent terms to the two-body potential. These terms in the UV14 plus TNI model were adjusted to give reasonable empirical saturation properties (recalculated by WFF to be $E_0=-16.6$ MeV at $\rho_0=0.157$ fm^{-3}, with $K_0=260$ MeV). However, the Hamiltonians with the UVII three-body potential were also required to give reasonable binding energies for the few-body nuclei ^{3}H and ^{4}He, and end up saturating nuclear matter with somewhat less binding at higher density. The interaction models, variational wave functions, ground-state calculations, and saturation properties are discussed in detail by WFF.

The $U(\rho,k)$ has been calculated here at densities of 0.1, 0.15, 0.2, 0.3, 0.4, and 0.5 fm^{-3}, and for momenta from 0.25 to 5 fm^{-1}. The calculations should be considered to be only qualitative above $\sim$4fm^{-1} because of the nonrelativistic nature of the Hamiltonian. One problem in comparing the momentum dependence of the models is the difference in saturation properties. At any given density, $U(\rho,k_F)$ is determined by the saturation curve for that model. To isolate the momentum dependence, I use a single $e(\rho,k_F)$ for the calculations, i.e., the $U(k)$ at any given density is calculated as in Eq. (5) except that the $e(\rho,k_F)$ defined by Eq. (2) is always taken from the UV14 plus TNI model. Thus at $k=k_F$, all the calculated curves are constrained to pass through the same point.

The results are shown in Fig. 1 for the UV14 plus TNI, UV14 plus UVII, and AV14 plus UVII models. The $e(\rho,k_F)$ points are also shown. The UV14 plus TNI model gives a very smooth momentum dependence that gradually steepens as the density increases. Results for the UV14 two-body potential alone (not shown) are virtually identical once the $e(\rho,k_F)$ adjustment is made, so the momentum dependence of the UV14 plus TNI model is determined strictly by the two-body potential. The UV14 plus UVII model gives a very similar momentum dependence at lower densities, but remains flatter and is notably more repulsive for low values of k at higher densities. The AV14 plus UVII model is slightly flatter than the UV14 models at lower density. At high density it is significantly more repulsive for momenta below k_F, and more attractive above k_F.

To better understand the influence of the explicit three-body potential, I also made a perturbative calculation at the higher densities for UV14 plus UVII by using the variational wave function optimized for the two-body potential alone. This perturbation calculation follows the UV14 plus TNI curve up to $\sim k_F$ but is more attractive at higher momenta. Comparing the curves in Fig. 1, it appears that the bulk of the difference between UV14 plus TNI and UV14 plus UVII at higher momenta is directly due to the three-body potential. This can be attributed to differences in the short-range structure of UVII and the effective TNI model. The greater repulsion at low momenta with UVII is due to nonperturbative changes in the wave function, primarily an enhancement of the long-range tensor correlations. The AV14 plus UVII model has even stronger tensor correlations, and more repulsion at low momenta.

In Fig. 1, I also show the simple parametrization for $U(\rho,k)$ suggested by Gale, Bertsch, and Das Gupta

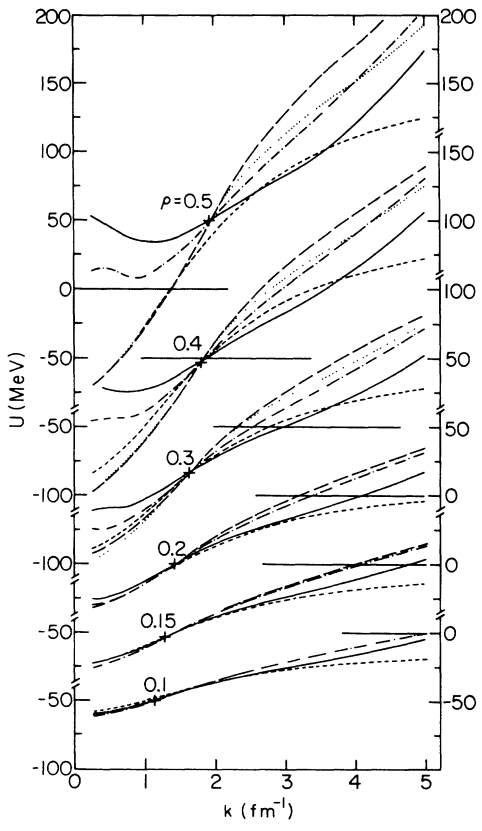

FIG. 1. The microscopic calculation of the single-particle potential $U(\rho,k)$ for Hamiltonians: UV14 plus TNI (dashed line), UV14 plus UVII (dash-dot line), AV14 plus UVII (solid line). The points $e(\rho,k_F)$ through which the curves are constrained to pass are shown by +'s. A perturbation calculation of UV14 plus UVII (dotted line) and the parametrization by Gale, Bertsch, and Das Gupta (short-dashed line) are also shown.

TABLE I. Parameters for fits to $U(\rho,k)$ for three Hamiltonians.

H	ρ (fm^{-3})	α (MeV)	β (MeV)	Λ (fm^{-1})
UV14 plus TNI	0.1	18.8	−76.7	3.14
	0.15	36.1	−108	2.87
	0.2	61.0	−142	2.75
	0.3	119	−213	2.64
	0.4	182	−286	2.46
	0.5	290	−368	2.67
UV14 plus UVII	0.1	16.9	−75.1	3.02
	0.15	32.5	−105	2.81
	0.2	55.4	−133	2.84
	0.3	105	−183	2.96
	0.4	192	−252	3.34
	0.5	318	−330	4.09
AV14 plus UVII	0.1	4.76	−62.3	2.86
	0.15	12.9	−82.5	2.63
	0.2	27.7	−102	2.61
	0.3	72.8	−138	3.07
	0.4	176	−211	4.31
	0.5	332	−311	6.00

(GBD),[7]

$$U(\rho,k)=a(\rho/\rho_0)+b(\rho/\rho_0)^{\sigma}+\frac{c(\rho/\rho_0)}{1+(k/\Lambda)^2}\left\langle\frac{1}{1+(k'/\Lambda)^2}\right\rangle, \quad (7)$$

where the parameters are $a=-145$ MeV, $b=203$ MeV, $\sigma=\frac{7}{6}$, $c=-75$ MeV, and $\Lambda=1.5k_{F_0}$, and the brackets indicate an expectation value. The momentum dependence is very similar to the UV14 plus TNI model up to k_F but is more attractive above k_F at all densities. It also has a corresponding equation of state very similar to UV14 plus TNI.

I have tried to fit the microscopic calculations with forms similar to Eq. (7). To get good quality fits, it is necessary to give a density dependence to the momentum

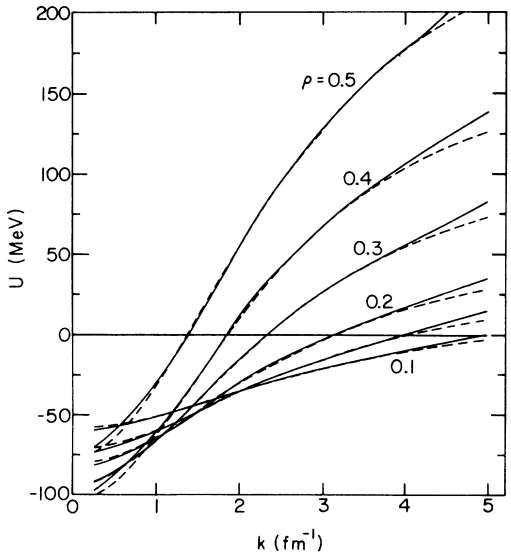

FIG. 2. The microscopic calculation of $U(\rho,k)$ for UV14 plus TNI (solid line) is compared to its fit from the parameters in Table I (dashed line).

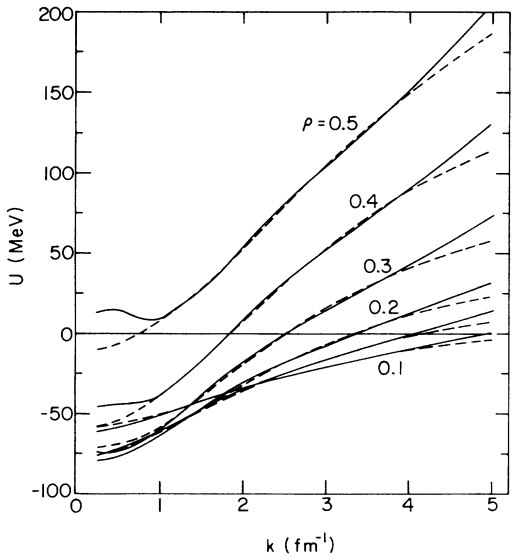

FIG. 3. The microscopic calculation of $U(\rho,k)$ for UV14 plus UVII (solid line) is compared to its fit from the parameters in Table I (dashed line).

scale Λ. In the simplest form, one can write

$$U(\rho,k)=\alpha(\rho)+\frac{\beta(\rho)}{1+[k/\Lambda(\rho)]^2}\ , \tag{8}$$

and use a least-squares method of fitting to determine $\alpha(\rho)$, $\beta(\rho)$, and $\Lambda(\rho)$ at each density. Th values so obtained are given in Table I and the corresponding fits are shown in Figs. 2–4. It is not possible with this form to fit the low momenta in the AV14 plus UVII or UV14 plus UVII models where they curve up at high density, so the fit has been made for momenta from 1 to 4 fm^{-1}. The values in Table I can be used as input to a simple interpolating routine for use in BUU calculations.

In summary, I have calculated the single-particle potential as a function of momentum and density in nuclear matter for several realistic Hamiltonians. The general similarity of the microscopic results for $U(\rho,k)$ to the GBD parametrization gives credence to their calculations. In turn, the success of BUU simulations with reasonable $U(\rho,k)$ in reproducing intermediate-energy heavy-ion collision data suggest there is no conflict with the equation of state predicted by Hamiltonians that fit nucleon-nucleon scattering data.

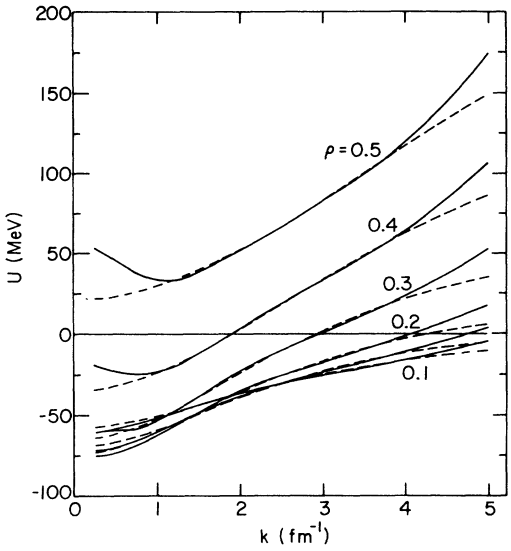

FIG. 4. The microscopic calculation of $U(\rho,k)$ for AV14 plus UVII (solid line) is compared to its fit from the parameters in Table I (dashed line).

I wish to thank S. Das Gupta for suggesting this problem and G. Bertsch, V. R. Pandharipande, and S. C. Pieper for their comments and advice. The calculations were performed at the National Magnetic Fusion Energy Computation Center, Livermore, California. This work was supported by the U. S. Department of Energy, Nuclear Physics Division under Contract W-31-109-ENG-38.

[1]G. F. Bertsch and S. Das Gupta, Phys. Rep. **160**, 189 (1988).
[2]R. Stock *et al.*, Phys. Rev. Lett. **49**, 1236 (1982); J. W. Harris *et al.*, *ibid.* **58**, 463 (1987).
[3]H. A. Gustafsson *et al.*, Phys. Rev. Lett. **52**, 1590 (1984); G. Buchwald *et al.*, *ibid.* **52**, 1594 (1984).
[4]H. Kruse, B. V. Jacak, and H. Stöcker, Phys. Rev. Lett. **54**, 289 (1985); J. J. Molitoris and H. Stöcker, Phys. Rev. C **31**, 346 (1985).
[5]B. Friedman and V. R. Pandharipande, Nucl. Phys. **A361**, 502 (1981).
[6]E. Baron, J. Cooperstein, and S. Kahana, Phys. Rev. Lett. **55**, 126 (1985).
[7]C. Gale, G. Bertsch, and S. Das Gupta, Phys. Rev. C **35**, 1666 (1987).
[8]J. Aichelin, A. Rosenhauer, and G. Peilert, H. Stoecker, and W. Greiner, Phys. Rev. Lett. **58**, 1926 (1987).
[9]R. B. Wiringa, V. Fiks, and A. Fabrocini, Phys. Rev. C **38**, 1010 (1988).
[10]B. Friedman and V. R. Pandharipande, Phys. Lett. **100B**, 205 (1981).
[11]I. E. Lagaris and V. R. Pandharipande, Nucl. Phys. **A359**, 331 (1981); **A359**, 349 (1981).
[12]R. B. Wiringa, R. A. Smith, and T. L. Ainsworth, Phys. Rev. C **29**, 1207 (1984).
[13]R. Schiavilla, V. R. Pandharipande, and R. B. Wiringa, Nucl. Phys. **A449**, 219 (1986).